DOI: 10.1002/ejic.201000863

# Hydrolytic Decomposition of Tetramethylammonium Bis(trifluoromethyl)aurate(I), $[NMe_4][Au(CF_3)_2]$: A Route for the Synthesis of Gold Nanoparticles in Aqueous Medium

David Zopes,[a] Silke Kremer,[a] Harald Scherer,[b] Lhoussaine Belkoura,[c]
Ingo Pantenburg,[a] Wieland Tyrra,[a] and Sanjay Mathur*[a]

**Keywords:** Gold / Nanoparticles / Hydrolysis / Plasmons

Monodisperse gold nanoparticles (AuNPs) were obtained by hydrolytic decomposition of a new molecular precursor, tetramethylammonium bis(trifluoromethyl)aurate(I), $[NMe_4][Au(CF_3)_2]$, which has been characterised by spectroscopic and single-crystal X-ray diffraction analyses. On account of the simple and high-yield synthesis, the title compound represents a versatile synthon and an alternative to the commonly used chloroauric acid ($HAuCl_4$).

## Introduction

Gold nanoparticles (AuNPs) attract a fascination in the field of nanotechnology,[1] mainly due to their appealing optical properties and the simplicity of the synthesis procedure, which have already been the focus of historical research on metal colloids.[1,2] Furthermore, these nanoparticles have already been transformed into commercial goods by incorporating them into glass matrices to obtain a distinct red coloration – caused by the plasmon resonance in nanoscopic gold clusters – seen in the stained glass windows of churches (e.g., "Purple of Cassius", made from gold in the presence of tin[3]). The tremendous interest in the applications of gold particles in modern nanotechnology emerges from their fundamentally new properties; for instance, AuNPs can act as carriers for the targeted delivery of drug and biomolecules inside cells. Similarly, their strong interaction with light enables a sensory mechanism in which the optical properties may change upon binding to certain molecules for the detection and quantification of analytes.[4] The most commonly used synthesis of gold nanoparticles involves the aqueous reduction of $HAuCl_4$ by sodium citrate.[5] The quest for a synthetic recipe that enables reproducible syntheses of Au nanoparticles with a precise control over size and shape has led to numerous modifications of the reduction of the precursor $HAuCl_4$.[6–8] Interestingly, a majority of the efforts deal with the modulation of growth parameters (reaction time, nature and concentration of reductants and so on) and growth kinetics (addition of capping agents, seed-mediated growth and so on) of AuNPs;[8] however, the development of new precursors for chemically controlled generation of gold nanoparticles has received somewhat less attention.[9] We report herein the synthesis and structural characterisation of (perfluoroalkyl)aurates(I) as potential synthons for the production of gold nanoparticles in aqueous media, which can be seen as a viable extension of the well-known $HAuCl_4$ routes.[5]

The efficient use of the reagent combination comprising a fluoride source plus trimethyl(perfluoroalkyl)silane has allowed us in recent years to prepare numerous perfluoroalkyl-metalate complexes of late transition metals as well as main-group elements that are characterised by their extreme reactivity[10–13] or stability.[14–16] (Trifluoromethyl)gold compounds, whereby the predominant numbers of the characterised derivatives contain gold in the trivalent oxidation state, have generally been known for more than 30 years.[17] The number of trifluoromethyl gold(I) compounds is limited to the examples of $AuCF_3{\cdot}RPF_2$,[18] $AuCF_3{\cdot}PR_3$[19] and $AuCF_3{\cdot}C{\equiv}NMe$;[20] however, no (perfluoroalkyl)aurate(I) has hitherto been described to the best of our knowledge.

The reagent combination $Me_3SiCF_3/F^-$ efficiently allows access to the synthesis of bis(trifluoromethyl)aurates(I) and avoids the use of alkylzinc or cadmium compounds.[18–22] We report here on the synthesis and structural characterisation of some bis(trifluoromethyl)aurates(I) and their reactivity in aqueous solutions, which has led to formations of monodisperse nanoparticles of Au, remarkably as aqueous dispersions.

---

[a] Department für Chemie, Lehrstuhl für Anorganische und Materialchemie, Universität zu Köln,
Greinstrasse 6, 50939 Köln, Germany
E-mail: sanjay.mathur@uni-koeln.de
[b] Institut für Anorganische und Analytische Chemie, Albert-Ludwigs-Universität Freiburg,
Albertstrasse 21, 79104 Freiburg i. Br, Germany
[c] Department für Chemie, Institut für Physikalische Chemie, Universität zu Köln,
Luxemburger Strasse 116, 50939 Köln, Germany

## Results and Discussion

### Synthesis and Characterisation of Bis(perfluoroalkyl)-aurates(I)

(Trifluoromethyl)gold(I) compounds are formed either as decomposition products of methyl(trifluoromethyl)gold(III) derivatives[17] or selectively formed through halide exchange reactions between AuX and $Cd(CF_3)_2$ complexes in the presence of suitable ligands such as phosphanes,[19] fluorophosphanes[18] or methyl isocyanide.[20]

The use of $Me_3SiCF_3$ as a reagent for the synthesis of $AuCF_3{\cdot}PR_3$ complexes has been reported in reactions of synthetically challenging alkoxy- or aryloxy-gold(I) compounds, $AuOR'{\cdot}PR_3$ [$R' = CH(CF_3)_2$, Ph].[23]

The synthesis of the bis(trifluoromethyl)aurates(I), $[Au(CF_3)_2]^-$, proceeds similar to the procedure reported for argentates,[15] platinates[14] and bismutates[11] (Scheme 1). Mechanistically, the hypercoordinated (hypervalent) trimethyl(trifluoromethyl) fluorosilicate anion that is formed in the elementary step[10] substitutes the chloride in AuCl to form highly volatile trimethylfluorosilane and sparingly soluble tetramethylammonium chloride. The intermediate species $\{[Au(CF_3)Cl]^-, AuCF_3{\cdot}EtCN\}$ then undergo a nucleophilic attack by a second equivalent of the trifluoromethyl nucleophile, thereby replacing either the chlorido or the propionitrilo ligand to finally yield $[NMe_4][Au(CF_3)_2]$ (Scheme 1).

$[NMe_4][Au(CF_3)_2]$ was obtained as a colourless solid in high yield and exhibited low sensitivity towards air and daylight. After storage in daylight for several months, the decomposition into elemental gold and gold(III) species was evident (by means of NMR and UV/Vis spectroscopic data) from which the tetrakis(trifluoromethyl)aurate(III) could be unambiguously identified. Quartets and septets in the $^{19}F$ NMR spectra – although of very low intensity – indicated tris(trifluoromethyl)gold(III) species of so far unknown composition.[24]

The $^{13}C$ NMR spectroscopic chemical shift of the bis(trifluoromethyl)aurate(I) anion in solution ($CD_3CN$) correlated well with the value reported for the isoelectronic derivative $Hg(CF_3)_2$. The coupling constants $^1J(^{19}F,^{13}C)$, $^3J(^{19}F,^{13}C)$ and $^4J(^{19}F,^{19}F)$ were also found to be comparable with those known for $Hg(CF_3)_2$ (Table 1). The quartet of quartet splitting caused by the $^1J(^{19}F,^{13}C)$ and $^3J(^{19}F,^{13}C)$ couplings of the $[Au(CF_3)_2]^-$ moiety is depicted in Figure 1.

Table 1. Comparison of the NMR spectroscopic data ($\delta$ in ppm, $J$ in Hz) of isoelectronic species $[Au(CF_3)_2]^-$ and $Hg(CF_3)_2$.[a]

| | $\delta(^{19}F)$ | $^1J$(F,C) | $^3J$(F,C) | $^4J$(F,F) | $\delta(^{13}C)$ |
|---|---|---|---|---|---|
| $[Au(CF_3)_2]^-$ | –28.5 | 347 | 19 | <2 | 163.0 |
| $Hg(CF_3)_2$ | –37.5 | 355 | 16 | 4.5 | 159.8 |

[a] $CD_3CN$, room temperature.

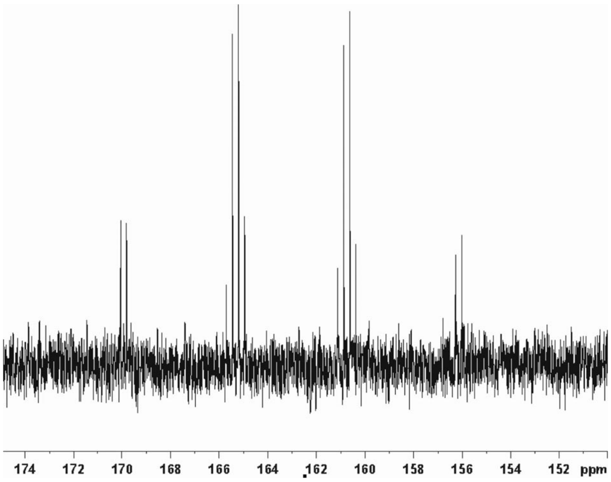

Figure 1. $^{13}C$ NMR spectrum of the $[Au(CF_3)_2]^-$ ion [$CD_3CN$; distortionless enhancement by polarization transfer, non decoupled, 30° pulse (deptnd30)].

An unexpected aurate(I), 1,1,1,4,5,5,5-heptafluoro-2,4-bis(trifluoromethyl)pent-2-ene-3-(trifluoromethyl)aurate(I) (Scheme 2), was identified with the help of correlated spectroscopy ($^{19}F,^{19}F$ and $^{19}F,^{13}C$), when a larger excess amount (>20%) of $Me_3SiCF_3$ was used, thus implying a similar reaction sequence as investigated for the formation of the 1,1,1,4,5,5,5-heptafluoro-2,4-bis(trifluoromethyl)pentide ion[25] in fluoride-mediated reactions of $Me_3SiCF_3$ with itself.

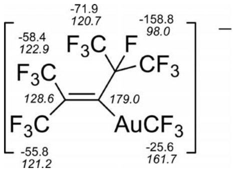

Scheme 2. Formula of 1,1,1,4,5,5,5 heptafluoro-2,4-bis(trifluoromethyl)-pent-2-ene-3-(trifluoromethyl)aurate(I) with $^{19}F$ and $^{13}C$ NMR spectroscopic chemical shifts ($^{13}C$ data printed in *italics*).

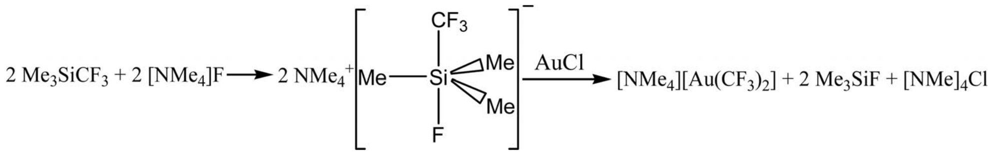

Scheme 1.

The $NMe_4^+$ cation was exchanged in a facile reaction with [PNP]I [PNP = bis(triphenylphosphoranylidene)ammonium] or [K(18-crown-6)]I to yield the corresponding aurates in nearly quantitative amounts.

### Molecular Structure of Bis(triphenylphosphoranylidene)ammonium Bis(trifluoromethyl)aurate(I), $[PNP][Au(CF_3)_2]$

The ion pair $[PNP][Au(CF_3)_2]$ (Figure 2) [C1–Au–C2 178.9(2)°; Au–C1 2.059(6) Å, Au–C2 2.072(6) Å] showed a quasilinear coordination for gold. These values and atomic arrangements are in good agreement with data for dimethylaurate(I), $[N(nBu)_4][Au(CH_3)_2]$ [mean value of Au–C bond length 2.075 Å; C–Au–C angle 178.2(2)°][26] and trifluoromethyl(triphenylphosphane)gold(I), $[Au(CF_3)(PPh_3)]$[27] [Au–C bond length 2.045(4) Å; C–Au–P angle 178.56(11)°].

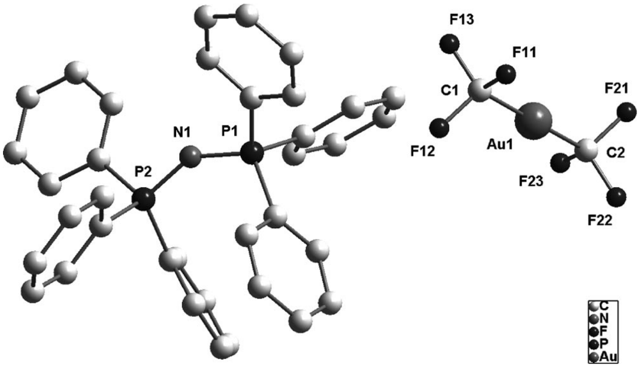

Figure 2. Molecular structure of the $[PNP][Au(CF_3)_2]$ ion pair.

In the crystal structure, anions are layered in channels formed by the bulky [PNP] cations without any significant F–H contacts (Figure 3). Thus, the bis(trifluoromethyl)aurate(I) may be added as a new candidate to the growing family of weakly coordinating anions (WCAs) that show no cation–anion interactions either in solution or in the solid state.[28]

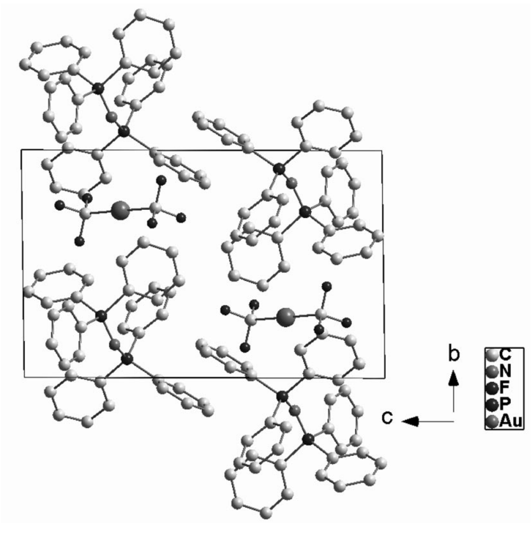

Figure 3. View of the unit cell along the crystallographic *a* axis.

Within the accessible range, the compound exhibited two irreversible oxidation waves at +0.73 and +1.05 V, which were tentatively assigned to $Au^{I}/Au^{II}$ and $Au^{II}/Au^{III}$ couples, respectively. No cathodic wave was detected up to –3.2 V, which indicated that within a large range of about 4 V the compound is stable (Figure 4).

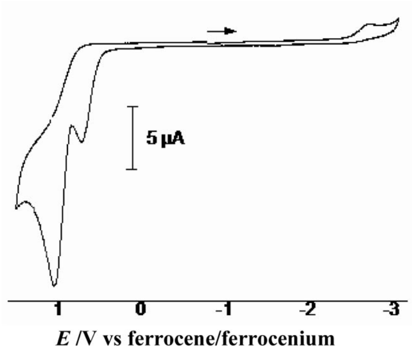

Figure 4. Cyclic voltammogram of $[NMe_4][Au(CF_3)_2]$ in MeCN/ $[N(nBu)_4]PF_6$ at 100 $mV\,s^{-1}$ scan rate; $T$ = 298 K. The small cathodic wave at about –2.7 V is due to an impurity in the solvent.

Kochi et al. reported an anodic oxidation wave for $[Au^{I}(CH_3)_2]^-$ of +0.498 V (converted into the ferrocene/ferrocenium couple) and a value of +0.822 V for the corresponding $Au^{III}$ compound $[Au(CH_3)_4]^-$.[26] Thus the first oxidation potential observed for $[Au(CF_3)_2]^-$ is about 0.23 V higher and reflects the electron-withdrawing effect of the $CF_3$ ligands in $[NMe_4][Au(CF_3)_2]$. A second anodic wave for $[Au^{I}(CH_3)_2]^-$ was not reported.

### Hydrolysis of $[NMe_4][Au(CF_3)_2]$

Although $[NMe_4][Au(CF_3)_2]$ is soluble in $CD_3OD$ without exhibiting any significant decomposition, the same attempt in $D_2O$ or $H_2O$ led to a rapid decomposition with evolution of bubbles ($CO_2$) accompanied by a colour change of the reaction mixture from grey through pale purple to red, which is characteristic of the formation and growth of gold nanoparticles.[2,5] After 30 min, no $^{19}F$ NMR spectroscopic evidence was found for any trifluoromethylgold(I) species in the solution. The decomposition products were identified to be $CO_2$ [precipitation of $BaCO_3$ upon bubbling the gas through a $Ba(OH)_2$ solution], $F^-$ that subsequently turned to $HF_2^-$[29] followed by $[SiF_6]^{2-}$ [$\delta(^{19}F)$ = –129.1 ppm; $\delta(^{29}Si)$ = –188 ppm; $^1J(^{29}Si,^{19}F)$ = 108 Hz] and $[BF_4]^-$ [$\delta(^{19}F)$ = –150.2 ppm; $\delta(^{11}B)$ = –1.4 ppm; $^1J(^{19}F,^{11}B) < 1$ Hz], the latter presumably being generated by the reaction with the glass wall of the NMR spectroscopy tube (Scheme 3). A further signal in the $^{19}F$ NMR spectrum that consisted of four lines of equal intensity as well as a quartet in the $^{11}$B NMR spectrum suggested the formation of $BF_3$·solvent adduct [$\delta(^{19}F)$ = –143.0 ppm; $\delta(^{11}B)$ = +0.3 ppm; $^1J(^{19}F,^{11}B)$ = 15 Hz]. No evidence was found for the formation of $CF_3H$. To decelerate the decomposition reaction and to elucidate the decomposition process, the hydrolysis was performed in a $CD_3CN/H_2O$ mixture ($v/v \approx 3{:}1$), which revealed a singlet in the $^{19}$F NMR spectra ($\delta$ = –21.0 ppm) and a quartet in the $^{13}$C NMR ($\delta$ = 145 ppm) spectra, assignable to $AuCF_3\cdot CD_3CN$ or possibly $AuCF_3\cdot H_2O$, although the formation of the latter appears to be unlikely. After a period of 5 d, a third signal that corresponded to trifluoromethylgold derivative was observed in the $^{19}$F and $^{13}$C NMR spectra, which upon comparison with published NMR spectroscopic data[24] suggested the formation of a mono(trifluoromethyl)gold(III) compound that was not characterised further. The formation of a formal Au$^{II}$ species with an Au–Au bond also cannot be excluded at this stage. These results denoted a selective hydrolysis by stepwise cleavage of F–C bonds and retention of one Au–$CF_3$ bond. An intermediately formed shortlived species $AuCF_3\cdot CO$ would be directly converted into the $CD_3CN$ adduct and $CO_2$, on account of the strong catalytic activity of gold (and its compounds) to oxidise CO.[30] A comparable conversion of a $CF_3$ group into a CO ligand has been recently reported for $[Pt(CF_3)_4]^{2-}$, which transformed under the influence of moisture into $[Pt(CF_3)_3(CO)]^-$.[31] A selective substitution of one fluorine atom of the $CF_3$ group with retention of the carbon–metal bond has been reported by D. Naumann et al.[32] in the treatments of $Cd(CF_3)_2$ complexes with Lewis acid–base couples. The consecutive reactions of the in situ generated HF with common glassware are also well documented.[29]

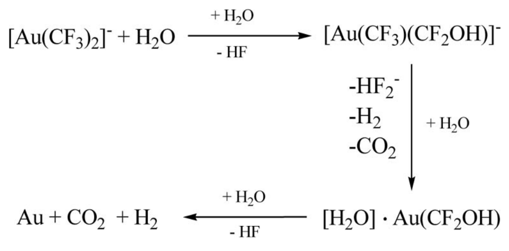

Scheme 3. Possible mechanistic pathways for the formation of AuNPs upon hydrolysis of $[NMe_4][Au(CF_3)_2]$ with aqueous ammonia.

To support these results, the reaction of $[NMe_4][Au(CF_3)_2]$ and trifluoroacetic acid anhydride (TFAA) was conducted to obtain further evidence for the proposed reaction mechanism. Upon treatment of a solution of $[NMe_4][Au(CF_3)_2]$ in $CD_3CN$ with an excess amount of TFAA, $^{19}$F NMR spectroscopic control exhibited after 10 min, besides the signal of the starting materials those of trifluoroacetyl fluoride $CF_3COF$ [$\delta(CF_3)$ = –75.5 ppm, d, $^3J(^{19}F,^{19}F)$ = 6.5 Hz, $^1J(^{19}F,^{13}C)$ = 283 Hz, $^2J(^{19}F,^{13}C)$ = 51 Hz, 3 F; $\delta$(COF) = +14.7 ppm, q, $^3J(^{19}F,^{19}F)$ = 6.5 Hz, $^1J(^{19}F,^{13}C)$ = 372 Hz, $^2J(^{19}F,^{13}C)$ = 96 Hz, 1 F], trifluoromethyl[difluoro(trifluoroacetato)methyl]aurate(I) $[Au(CF_3)(CF_2OCOCF_3)]^-$ [$\delta(CF_3)$ = –28.6 ppm, t, $^4J(^{19}F,^{19}F) \approx$ 1.5 Hz, $^1J(^{19}F,^{13}C)$ = 346 Hz, 3 F; $\delta(CF_2)$ = –43.0 ppm, q, $^4J(^{19}F,^{19}F) \approx$ 1.5 Hz, $^1J(^{19}F,^{13}C)$ = 337 Hz, 2 F; $\delta(OCOCF_3)$ = –77.2 (–77.17) ppm, s, $^1J(^{19}F,^{13}C)$ = 293 Hz, 3 F] and bis[difluoro(trifluoroacetato)methyl]aurate(I) $[Au(CF_2OCOCF_3)_2]^-$ [$\delta(CF_2)$ = –42.8 ppm, s, $^1J(^{19}F,^{13}C)$ = 336 Hz, $^4J(^{19}F,^{13}C) \approx$ 2 Hz, 4 F; $\delta(OCOCF_3)$ = –77.2 (–77.21) ppm, s, $^1J(^{19}F,^{13}C)$ = 293 Hz, 6 F].

After prolonged reaction periods, the resonances of trifluoromethyl[difluoro(trifluoroacetato)methyl]aurate(I) $[Au(CF_3)(CF_2OCOCF_3)]^-$ vanished, whereas the signal intensities of $CF_3COF$ and bis[difluoro(trifluoroacetato)methyl]aurate(I) $[Au(CF_2OCOCF_3)_2]^-$ increased. Therefore, $^{13}$C NMR spectroscopic chemical shifts for the latter could be provided [$^{19}$F,$^{13}$C heteronuclear single-quantum coherence (HSQC) experiments, optimised for 340 Hz; $^{19}$F,$^{13}$C heteronuclear multiple-bond correlation (HMBC) experiments, optimised for 30 Hz] to be $\delta$ = 159.4 ($CF_2$), 153.1 (OCO) and approximately 111.5 ppm ($OCOCF_3$). On the basis of above observation, we suggest that intermediately formed CO acts as a reducing reagent under the influence of water, whereas ammonia became the reagent of choice to eliminate unwanted byproducts (Scheme 3).

## Formation of AuNPs

In addition to the described and characterised byproducts, colloidal gold was obtained after the hydrolysis of $[NMe_4][Au(CF_3)_2]$. The purple-coloured solution that contained AuNPs was investigated by UV/Vis spectra to elucidate time-dependent particle growth. The scanning and transmission electron micrographs provided insight into particle morphology and size distribution. Figure 5 (a) shows the kinetic behaviour of the UV/Vis absorption measurement for a 2.0 mM aqueous solution of $[NMe_4][Au(CF_3)_2]$. The spectroscopic data showed that nucleation of the AuNPs began after 20 min with a maximal absorption around $\lambda_{max}$ = 515 nm and a low intensity (ca. 0.5). The absorption maxima gradually showed a redshift that indicated the particle growth by ripening processes.[33] The reaction was found to be over after approximately 120 min, as no further shift or colour change was observed.

Figure 5 (b) shows SEM image of particles formed after 120 min with an average particle size of around 28.7 nm ($\sigma \approx$ 17.7%). As expected, the unprotected particles (no surface coating) tend to assemble and agglomerate. The agglomeration of NPs was augmented at higher precursor concentration, which was corroborated by the observed redshift of the absorption maxima in the UV/Vis spectra and the increase in the polydispersity (Figure 6). Initially, monodisperse AuNPs with an average size of 12.0 nm and a size distribution of around 12.5% are formed (Figure 7), which grew in size in concentrated (4.0 mM) solutions to produce AuNPs of average particle size (52.5 nm) with a substantially broader size distribution of 25.5% (Figure 6).

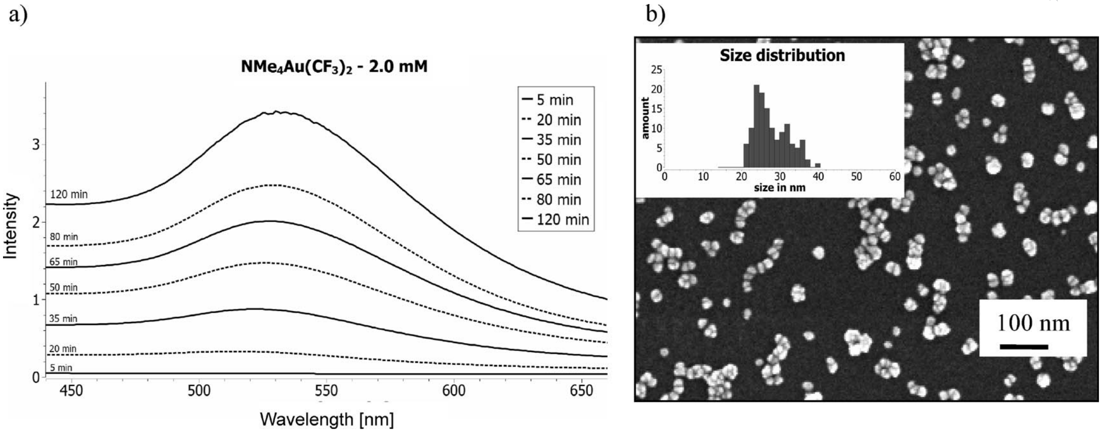

Figure 5. Time-dependent UV/Vis measurements (a) and SEM image (120 min) (b) including size distribution to control the kinetic of the growth of the AuNPs starting from 2.0 mm solution of $[NMe_4][Au(CF_3)_2]$ precursor.

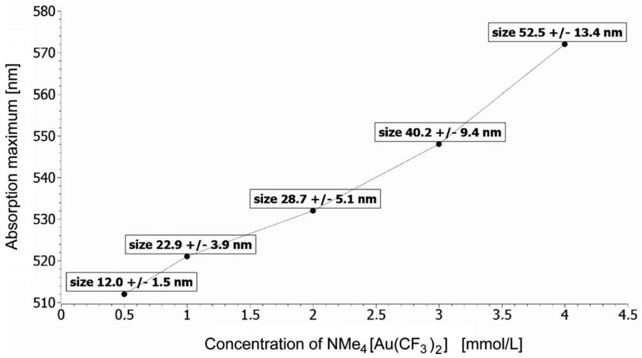

Figure 6. Influence of the precursor concentration on the resulting size of AuNPs monitored by UV/Vis absorption spectra. The average particle size obtained from the TEM and SEM analyses of the corresponding samples are given in the boxes shown along the plotted numerical values.

The stability of AuNP dispersions could be enhanced by reduction of the precursor concentration. For instance, NPs obtained from 0.5 mm aliquots were stable for more than two weeks and only very slow agglomeration process was observed in the UV/Vis measurements (Figure 7). This precursor concentration is comparable to the procedure reported by Turkevich and co-workers when using $HAuCl_4$ as starting material.[5]

The formation of HF over the course of the decomposition reaction and its further reaction with the glass to generate $[SiF_6]^{2-}$ and $[BF_4]^-$ prompted us to use $NH_3$ as a scavenger for HF. As expected, the addition of a small amount of $NH_3$ induced the formation of $NH_4F$ ($^{19}F$ NMR spectroscopic evidence), thereby accelerating the decomposition reaction and reducing the reaction time from 120 to 20 min.

Figure 8 shows the AuNPs obtained after this modification for a concentration of 0.5 mm solution of $[NMe_4][Au(CF_3)_2]$. Evidently, a chemically controlled (formation of $NH_4F$) decomposition of precursor due to the addition of $NH_3$ led to a fast nucleation step, thereby inhibiting particle growth by ripening and aggregative mechanisms. As a result, the obtained particles were nearly monodispersed (size distribution, 8.3%) with an average particle size of 9.7 nm.

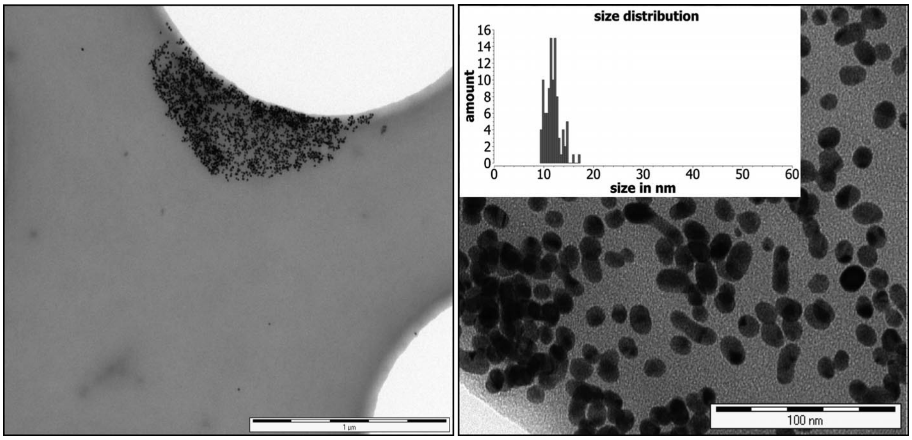

Figure 7. TEM images and analysed size dispersion in AuNPs (at two different magnifications) obtained by a reduced precursor concentration of 0.5 mm $[NMe_4][Au(CF_3)_2]$.

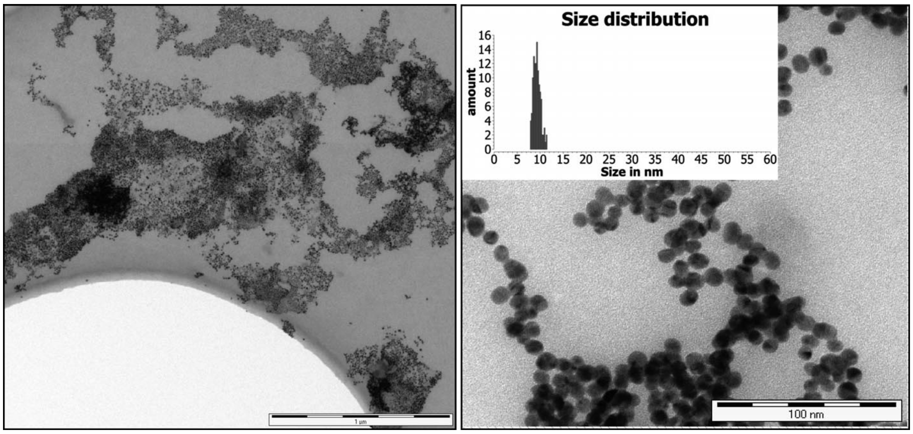

Figure 8. TEM images and analysed size distribution of AuNPs (at two different magnifications) obtained by a precursor concentration of 0.5 mM and few amounts of $NH_3$.

## Conclusion

We have reported a room-temperature synthesis of monodisperse AuNPs by the hydrolysis of a new gold precursor, $[NMe_4][Au(CF_3)_2]$. Mechanistic investigations by time-dependent NMR and UV/Vis spectroscopic data revealed that the precursor-to-nanoparticle transformation is governed by a cascade of chemical reactions that can be explained at the molecular level. The simplicity of the precursor activation and the possibility of controlling its decomposition kinetics by addition of, for example, $NH_3$ to scavenge in situ formed HF, enabled a size-controlled synthesis of gold nanoparticles.

## Experimental Section

**General:** All experiments were carried out in a dry nitrogen or argon atmosphere in carefully dried reaction vessels using Schlenk techniques. Solvents were purified by reported methods.[34] AuCl,[35] $[NMe_4]F$[36] and [PNP]I[37] were synthesised according to literature procedures. [K(18-crown-6)]I was prepared from a 1:1 reaction of KI and the crown ether in an acetone dichloromethane mixture. NMR spectra were recorded with a Bruker AVANCE II 300 spectrometer at 298 K; NMR spectrosopic frequencies (external standards): $^{13}C$: 75.5 MHz (TMS), $^{19}F$: 282.4 MHz ($CCl_3F$), $^{1}H$: 300.1 MHz (TMS); positive shifts denote downfield resonances. Data collection to solve the structure of 1,1,1,4,5,5,5-heptafluoro-2,4-bis(trifluoromethyl)pent-2-ene-3-(trifluoromethyl)aurate(I) were carried out with a Bruker Avance 400 spectrometer at ambient temperature. Electrochemical experiments were carried out in 0.1 M $[N(nBu)_4]PF_6$ solutions with a three-electrode configuration (glassy carbon electrode, Pt counter electrode, Ag/AgCl reference) and an Autolab PGSTAT30 potentiostat and function generator. The ferrocene/ferrocenium couple ($FeCp_2/FeCp_2^+$) served as internal reference. Negative ESI mass spectra in MeCN solutions were carried out with a Finnigan MAT 900 apparatus with a flow rate of $2\,\mu L\,min^{-1}$. Visible decomposition points were determined with a HWS Mainz 2000 apparatus. C, H and N analyses were carried out with a HEKAtech Euro EA 3000 apparatus. The obtained AuNPs were characterised by UV/Vis spectroscopy (Perkin–Elmer), transmission electron microscopy (Zeiss) and a scanning electron microscope (FEI).

**Tetramethylammonium Bis(trifluoromethyl)aurate(I):** Solid $[NMe_4]F$ (0.77 g; 8.28 mmol) was added to a well-stirred solution of $Me_3SiCF_3$ (1.487 mL, 9.93 mmol) in dry dimethoxyethane (15 mL) at –60 °C, and the reaction mixture was slowly warmed to –30 °C. At this temperature, AuCl (0.85 g, 4.14 mmol) was added. After a while, $[NMe_4]Cl$ together with traces of elemental gold begin to precipitate as a pale grey solid. The reaction mixture was allowed to reach room temperature overnight. All volatile components were removed in vacuo to obtain a waxy residue, which was washed several times with small portions of *n*-pentane and dried in vacuo. $[NMe_4][Au(CF_3)_2]$ was extracted from the powdery ochre raw material by using dichloromethane with a Soxhlet apparatus and a bath temperature that did not exceed 80 °C. Extraction was terminated after 9 h. After removing the main quantity of the solvent by use of a rotary evaporator, the colourless remainder was dried in vacuo to give 1.02 g (2.48 mmol) $[NMe_4][Au(CF_3)_2]$ in 60% yield as colourless crystals; m.p. 174–178 °C (glass capillary). $^{19}F$ NMR (282.4 MHz, $CD_3CN$, 298 K, $CCl_3F$): $\delta$ = –28.5 [s, $^1J$(F,C) = 347 Hz, $^3J$(F,C) = 19 Hz, $^4J$(F,F) = 2 Hz] ppm. $^{13}C\{^1H\}$ NMR (75.5 MHz, $CD_3CN$, 298 K, TMS): $\delta$ = 163.0 {qq, $^1J$(F,C) = 347 Hz, $^3J$(F,C) = 19 Hz, $[Au(CF_3)_2]^-$}, 55.3 {"t", $^1J$(C,N) = 4 Hz, $[NMe_4]^+$} ppm. $^1H$ NMR (300.1 MHz, $CD_3CN$, 298 K, TMS): $\delta$ = 3.12 {"t", $^2J$(H,N) = 0.6 Hz, $[NMe_4]^+$} ppm. NMR spectroscopic data recorded in $CD_3OD$ did not differ significantly. MS $(ESI)^-$: *m*/*z* (%) = 335.0 (100) $[Au(CF_3)_2]^-$. $C_6H_{12}AuF_6N$ (409.12): calcd. C 17.61, H 2.96, N 3.42; found C 18.22 , H 3.45, N 3.55.

**Bis(triphenylphosphoranylidene)ammonium Bis(trifluoromethyl)aurate(I) $[PNP][Au(CF_3)_2]$ and Potassium(18-crown-6) Bis(trifluoromethyl)aurate(I) $[K(18\text{-crown-}6)][Au(CF_3)_2]$:** [PNP]I (0.67 g, 1.0 mmol) and [K(18-crown-6)]I} (0.43 g, 1.0 mmol) dissolved in 10 mL of EtCN were added to a solution of $[NMe_4][Au(CF_3)_2]$ (ca. 1.0 mmol) that was prepared as described above. $[NMe_4]I$ precipitated spontaneously after mixing both solutions; it was filtered off and the resulting solution was evaporated to dryness. After washing with *n*-pentane, colourless crystals of $[PNP][Au(CF_3)_2]$ {[K(18-crown-6)]$[Au(CF_3)_2]$} were grown upon storing a $CH_2Cl_2/Et_2O$ mixture for several days at –20 °C. The crystals were isolated in better than 95% yield in both cases. $C_{38}H_{30}AuF_6NP_2$ (873.56): calcd. C 52.25, H 3.46, N 1.60; found C 52.07, H 3.99, N 1.63; m.p. 198–200 °C (glass capillary). $C_{14}H_{24}AuF_6KO_6$ (638.39): calcd. C 26.34, H 3.79, N 0.00; found C 26.91, H 4.51, N 0.75; m.p. (onset of decomposition) 194 °C (glass capillary). $^{19}F$ and $^{13}C$ NMR spectra of the anion matched with those of $[NMe_4][Au(CF_3)_2]$ described above. $^1H$ and $^{13}C$ NMR spectroscopic data of the [PNP] and [K(18-crown-6)] cations matched with previously published values.[38]

**AuNPs:** The [$NMe_4$][$Au(CF_3)_2$] was purified from elemental gold residues by extracting the product in dichloromethane with a Soxhlet apparatus. The pure [$NMe_4$][$Au(CF_3)_2$] was stored under argon and dark conditions to avoid any premature decomposition. The complex was hydrolysed under continuous stirring at different concentrations (0.5–4.0 mM). A small amount of ammonia was added to accelerate the decomposition. The reaction mixture turned red after 6 min and the reaction monitored by UV/Vis spectra was completed after 20 min. The obtained particles were characterised by UV/Vis spectroscopy and TEM and SEM measurements.

**Single-Crystal X-ray Diffraction Study:** Single crystals of [PNP][$Au(CF_3)_2$] were obtained upon cooling saturated $CH_2Cl_2$ solutions to approximately –25 °C over several weeks. Data collection for X-ray crystal-structure determination were performed with a STOE IPDS II diffractometer using graphite-monochromated Mo-$K_\alpha$ radiation ($\lambda$ = 71.073 pm). The data were corrected for Lorentz and polarisation effects. A numerical absorption correction based on crystal-shape optimisation was applied for all data.[39] The programs used in this work are Stoe's X-Area,[40] including X-RED and X-Shape for data reduction and absorption correction[41] and the WinGX suite of programs,[42] including SIR-92[43] and SHELXL-97[44] for structure solution and refinement. The hydrogen atoms were placed in idealised positions and constrained to ride on their parent atom. The last cycles of refinement included atomic positions for all atoms, anisotropic thermal parameters for all non-hydrogen atoms and isotropic thermal parameters for all hydrogen atoms. Materials for publication were prepared using DIAMOND.[45]

CCDC-785918 contains the supplementary crystallographic data for this paper. These data can be obtained free of charge from The Cambridge Crystallographic Data Centre via www.ccdc.cam.ac.uk/data_request/cif.

**Crystal Data for [PNP][$Au(CF_3)_2$]:** $C_{38}H_{30}NP_2F_6Au$: 873.56 $g\,mol^{-1}$; diffractometer IPDS-II, $T$ = 170(2) K; $2\theta_{max}$ = 54.8°; $0° \leq \omega \leq 180°$, $\phi$ = 0°, $0° \leq \omega \leq 58°$, $\phi$ = 90°, $\Delta\omega$ = 2°, 119 images; $-12 \leq h \leq 12$, $-13 \leq k \leq 13$, $-21 \leq l \leq 21$; $\rho_{calcd.}$ = 1.689 $g\,cm^{-3}$; 16920 measured reflections of which 7502 were symmetrically independent; $R_{int}$ = 0.0526; $F(000)$ = 856; $\mu$ = 4.437 $mm^{-1}$; triclinic, $P\bar{1}$ (no. 2), $a$ = 990.7(1) pm, $b$ = 1081.6(1) pm, $c$ = 1717.5(2) pm, $\alpha$ = 85.31(1)°, $\beta$ = 74.83(1)°, $\gamma$ = 75.28(1)°, $V$ = 1717.7(7)$\times 10^6$ $pm^3$, $Z$ = 2; $R_1/wR_2$ for 6033 reflections with [$I_o > 2\sigma(I_o)$]: 0.0367/0.0866, for all data: 0.0506/0.1004; $S_{all}$ = 1.032.

## Acknowledgments

The authors would like to thank the University of Cologne and the European Union (EU), project "NANOMMUNE" funded within the framework of the NMP call of the seventh framework programme (FP7-NMP-2007-SMALL-1, grant number 214281) for providing the infrastructure and financial assistance. Thanks are due to Professor Dr. Dieter Naumann for valuable discussions. We express our gratitude to our advanced students Gulara Hamidova, Iana Sterman, Sabine Grupe and Stefan Schüller for doing some part of the experimental work. We are indebted to Professor Dr. Axel Klein for interpreting the cyclic voltammetry data, to Dr. Mathias Schäfer (Institut für Organische Chemie) for recording the ESI mass spectra and to Osman Arslan for the TEM measurements.

---

[1] a) M. Faraday, *Philos. Trans. R. Soc. London* **1857**, *147*, 145; b) S. A. Edwards, *The Nanotech Pioneers*, Wiley, USA, **2006**, ISBN 978-3527312900.

[2] P. P. Edwards, J. M. Thomas, *Angew. Chem. Int. Ed.* **2007**, *46*, 5480–5486.

[3] G. Schmid, *Cluster and Colloids: From Theory to Applications*, VCH Verlagsgesellschaft, Weinheim, Germany, **1994**.

[4] A. R. Sperling, P. R. Gil, F. Zhang, M. Zanella, W. J. Parak, *Chem. Soc. Rev.* **2008**, *37*, 1896–1908.

[5] J. Turkevich, P. C. Stevenson, J. Hillier, *J. Phys. Chem.* **1953**, *57*, 670–673.

[6] J. Kimling, M. Maier, B. Okenve, V. Kotaidis, H. Ballot, A. Plech, *J. Phys. Chem. B* **2006**, *110*, 15700–15707.

[7] M. Brust, M. Walker, D. Bethell, D. J. Schiffrin, R. Whyman, *J. Chem. Soc., Chem. Commun.* **1994**, 801–802.

[8] M.-C. Daniel, D. Astruc, *Chem. Rev.* **2004**, *104*, 293–346.

[9] a) S. D. Bunge, T. J. Boyle, T. J. Headley, *Nano Lett.* **2003**, *3*, 901–905; b) J. Zeng, Y. Ma, U. Jeong, Y. Xia, *J. Mater. Chem.* **2010**, *20*, 2290–2301; c) T. Placido, R. Comparelli, F. Giannici, P. D. Cozzoli, G. Capitani, M. Striccoli, A. Agostiano, M. L. Curri, *Chem. Mater.* **2009**, *21*, 4192–4202.

[10] N. Maggiarosa, W. Tyrra, D. Naumann, N. V. Kirij, Yu. L. Yagupolskii, *Angew. Chem.* **1999**, *111*, 2392–2393; *Angew. Chem. Int. Ed.* **1999**, *38*, 2252–2253.

[11] W. Tyrra, D. Naumann, N. V. Kirij, A. A. Kolomeitsev, Yu. L. Yagupolskii, *J. Chem. Soc., Dalton Trans.* **1999**, 657–658.

[12] N. V. Kirij, Yu. L. Yagupolskii, N. Maggiarosa, W. Tyrra, D. Naumann, *J. Fluorine Chem.* **2001**, *112*, 213–218.

[13] N. V. Pavlenko, L. A. Babadzhanova, I. I. Gerus, Yu. L. Yagupolskii, W. Tyrra, D. Naumann, *Eur. J. Inorg. Chem.* **2007**, 1501–1507.

[14] D. Naumann, N. V. Kirij, N. Maggiarosa, W. Tyrra, Yu. L. Yagupolskii, M. S. Wickleder, *Z. Anorg. Allg. Chem.* **2004**, *630*, 746–751.

[15] a) S. Aboulkacem, W. Tyrra, I. Pantenburg, *J. Chem. Crystallogr.* **2006**, *36*, 141–145; b) W. Tyrra, D. Naumann, *J. Fluorine Chem.* **2004**, *125*, 823–830.

[16] a) W. Tyrra, D. Naumann, Yu. L. Yagupolskii, *J. Fluorine Chem.* **2003**, *123*, 183–187; b) W. Tyrra, N. V. Kirij, D. Naumann, Yu. L. Yagupolskii, *J. Fluorine Chem.* **2004**, *125*, 1435–1438.

[17] H. Schmidbauer, A. Schier, *Science Synthesis* **2004**, *3*, 691–761.

[18] A. Gräfe, T. Kruck, *J. Organomet. Chem.* **1996**, *506*, 31–35.

[19] a) R. D. Sanner, J. H. Satcher Jr., M. W. Droege, *Organometallics* **1989**, *8*, 1498–1506; b) H. K. Nair, J. A. Morrison, *J. Organomet. Chem.* **1989**, *376*, 149–164.

[20] N. H. Dryden, J. G. Shapter, L. L. Coatsworth, P. R. Norton, R. J. Puddephatt, *Chem. Mater.* **1992**, *4*, 979–981.

[21] H. Lange, D. Naumann, *J. Fluorine Chem.* **1984**, *26*, 435–444.

[22] H. Lange, D. Naumann, *J. Fluorine Chem.* **1984**, *26*, 1–18.

[23] Y. Usui, J. Noma, M. Hirano, S. Komiya, *Inorg. Chim. Acta* **2000**, *309*, 151–154.

[24] E. Bernhardt, M. Finze, H. Willner, *J. Fluorine Chem.* **2004**, *125*, 967–973.

[25] W. Tyrra, M. M. Kremlev, D. Naumann, H. Scherer, H. Schmidt, B. Hoge, I. Pantenburg, Yu. L. Yagupolskii, *Chem. Eur. J.* **2005**, *11*, 6514–6518.

[26] D. Zhu, S. V. Lindeman, J. K. Kochi, *Organometallics* **1999**, *18*, 2241–2248.

[27] U. Flörke, H.-J. Haupt, P. G. Jones, *Acta Crystallogr., Sect. C* **1996**, *52*, 609–611.

[28] I. Krossing, I, Raabe, *Angew. Chem.* **2004**, *116*, 2116–2142; *Angew. Chem. Int. Ed.* **2004**, *43*, 2066–2090.

[29] K. O. Christe, W. W. Wilson, *J. Fluorine Chem.* **1990**, *46*, 339–342.

[30] A. S. K. Hashmi, G. L. Hutchings, *Angew. Chem.* **2006**, *118*, 8064–8105; *Angew. Chem. Int. Ed.* **2006**, *45*, 7896–7936.

[31] S. Martinez-Salvador, B. Menjón, J. Forniés, A. Martín, I. Usón, *Angew. Chem.* **2010**, *122*, 4382–4385; *Angew. Chem. Int. Ed.* **2010**, *49*, 4286–4289.

[32] a) D. Naumann, R. Möckel, W. Tyrra, *Angew. Chem.* **1994**, *106*, 325–326; *Angew. Chem. Int. Ed. Engl.* **1994**, *33*, 323–325; b) R. Möckel, W. Tyrra, D. Naumann, *J. Fluorine Chem.* **1995**, *73*, 229–235; c) W. Tyrra, D. Naumann, *Can. J. Chem.* **1991**, *69*, 327–333.

[33] a) S. Link, M. A. El-Sayed, *J. Phys. Chem. B* **1999**, *103*, 8410–8426; b) C. Noguez, *J. Phys. Chem. C* **2007**, *111*, 3806–3819.

[34] D. D. Perrin, W. L. F. Armarego, D. R. Perrin, *Purification of Laboratory Chemicals*, 2nd ed., Pergamon Press, Oxford, **1980**.

[35] O. Glemser, H. Sauer, in: *Handbuch der Präparativen Anorganischen Chemie*, 2$^{nd}$ ed. (Ed.: G. Brauer), Ferdinand Enke, Stuttgart, Germany, **1962**, p. 927.

[36] A. A. Kolomeitsev, F. U. Seifert, G.-V. Röschenthaler, *J. Fluorine Chem.* **1995**, *71*, 47–49.

[37] J. K. Ruff, W. J. Schlientz, *Inorg. Synth.* **1974**, *15*, 84–96.

[38] Z.-H. Choi, W. Tyrra, A. Adam, *Z. Anorg. Allg. Chem.* **1999**, *625*, 1287–1292.

[39] *X-Shape 1.06*, Crystal Optimisation for Numerical Absorption Correction (C), STOE & Cie GmbH, Darmstadt, Germany, **1999**.

[40] *X-Area 1.16*, Stoe & Cie GmbH, Darmstadt, Germany, **2003**.

[41] *X-RED 1.22*, Stoe Data Reduction Program (C), Stoe & Cie GmbH, Darmstadt, Germany, **2001**.

[42] L. J. Farrugia, *J. Appl. Crystallogr.* **1999**, *32*, 837–838.

[43] A. Altomare, G. Cascarano, C. Giacovazzo, A. Guagliardi, *J. Appl. Crystallogr.* **1993**, *26*, 343–350.

[44] G. M. Sheldrick, *SHELXL-97*, *Programs for Crystal Structure Analysis*, University of Göttingen, Germany, **1997**.

[45] K. Brandenburg, *Diamond*, version 2.1e, Crystal Impact GbR, Bonn, Germany, **1996**–**2001**.

Received: August 10, 2010